Supplemental Material to "Ultrafast electronic band gap control in an excitonic insulator"

Selene Mor,[1] Marc Herzog,[1] Denis Golež,[2] Philipp Werner,[2] Martin Eckstein,[3] Naoyuki Katayama,[4] Minoru Nohara,[5] Hide Takagi,[6,7] Takashi Mizokawa,[8] Claude Monney,[9,*] and Julia Stähler[1]

[1] *Fritz-Haber-Institut der MPG, Faradayweg 4-6, 14195 Berlin, Germany*
[2] *Dept. of Physics, Univ. of Fribourg, 1700 Fribourg, Switzerland*
[3] *Max Planck Research Dept. for Structural Dynamics, Univ. of Hamburg-CFEL, 22761 Hamburg, Germany*
[4] *Dept. of Physical Science and Engineering, Nagoya Univ., 464-8603 Nagoya, Japan*
[5] *Research Institute for Interdisciplinary Science, Okayama Univ., Okayama 700-8530, Japan*
[6] *Max Planck Institute for Solid State Research, 70569 Stuttgart, Germany*
[7] *Dept. of Physics, Univ. of Tokyo, 113-8654 Tokyo, Japan*
[8] *Dept. of Applied Physics, Waseda Univ., 169-8555 Tokyo, Japan*
[9] *Institute of Physics, Univ. of Zurich, Winterthurerstrasse 190, 8057 Zurich, Switzerland*

(Dated: June 20, 2017)

Experimental details

TNS single crystalline samples were prepared by reacting the elementals nickel, tantalum and selenium with a small amount of iodine in a evacuated quartz tube. The tube was slowly heated and kept with a temperature gradient from 950°C to 850°C for 7 days, followed by slow cooling. Single crystalline samples with a typical size of 0.04 x 1 x 10 mm^3 were obtained in the cooler end.

For trARPES, the samples were cleaved *in situ* at room temperature under ultrahigh vacuum conditions (1.6×10^{-10} mbar) and then slowly cooled down to 110 K using liquid N_2. TNS was optically excited by the p-polarized, fundamental output ($h\nu_{pump} = 1.55$ eV) of a regeneratively amplified Ti:Sa laser system working at a repetition rate of 40 kHz. The photoinduced changes to the electronic structure along the Ni chain direction of TNS were probed by time-delayed p-polarized probe pulses ($h\nu_{probe} = 6.2$ eV), generated by frequency quadrupling of the fundamental. The two-photon photoemission signal of TNS at high kinetic energies represents a cross correlation of the Gaussian pump and probe laser pulses and was used to estimate an upper limit for the time resolution of 110 fs. The photoelectrons were detected by a hemispherical analyzer (SPECS Phoibos 100) held at a bias voltage of 0.5 V with respect to the sample holder. The energy resolution of 86 meV is obtained as root sum squared of the UV pulse bandwidth (25 meV) and the instrument resolution (82 meV) estimated *in situ* from the low-energy secondary electron cut-off of a direct photoemission spectrum of the metallic sample holder. Due to the high statistics of our raw data, it was possible to resolve *relative* energy shifts of only few meV. PE spectra are plotted as a function of energy with respect to the equilibrium Fermi level $E - E_F = E_{kin} - h\nu_{probe} + \Phi$. Φ is the work function. E_F was determined independently on the metallic sample holder, which was in direct electrical contact with the sample. We can neglect sample charging as the origin of the observed transient spectral shifts as (i) no *rigid* shift of the angle-resolved PE spectra was observed (parts of the spectrum shift up, others down) and (ii) the low-energy secondary electron cut-off remains unchanged. This is exemplified in Fig. 1, where we compare EDCs at Γ showing the whole ARPES spectra measured before $\Delta t = 0$ fs and at $\Delta t = 185$ fs (for a fluence of 0.12 mJ/cm^2) at 110 K. While the peaks of the lower and upper VB are transiently modified by the pump pulse, this shows that the low-energy cut-off (at a binding energy of about -0.8 eV) remains unchanged. This has been checked for different fluences and at different time delays.

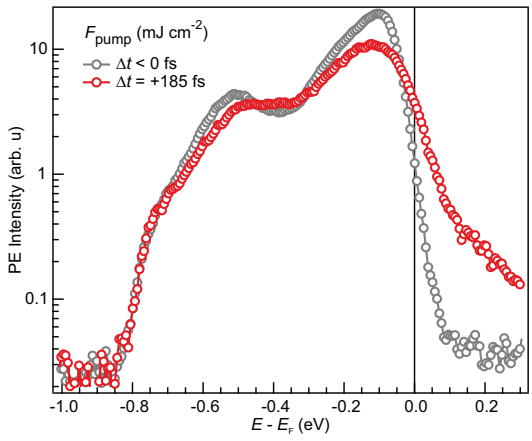

FIG. 1. EDCs at Γ before (empty grey) and at 185 fs (empty red) after photoexcitation for a fluence of 0.12 mJ/cm^2.

Experimental data analysis

EDCs were fitted with a sum of three Gaussian peaks multiplied by the Fermi-Dirac occupation distribution

(FDD) and convoluted with another Gaussian to account for the energy resolution as exemplarily shown in Fig. 2. The Gaussian peak at higher binding energy fits to the lower VB, while the sum of the other two Gaussians is used to reproduce the asymmetric shape of the upper VB. The EDC at $\Delta t = 365$ fs (solid red markers) in Fig. 2 clearly shows the downward shift of the upper flat top VB upon strong photoexcitation. This delayed downshift is sufficiently pronounced to be directly seen in the raw PE data, as evidenced by the normalized EDCs for different time delays before (empty grey) and after (solid red) photoexcitation. The time-dependent energetic position of the intensity maximum of the combined peak was used as a measure for the transient shift of the upper VB[1]. Since the energy shift of both peaks is sufficiently strong to be seen by eye in the raw data, different fit functions (not shown, e.g. two Gaussians w/o FDD and three Gaussians w/ FDD) yield qualitatively the same result. Tests demonstrate that apparent band shifts due to FDD broadening can only account for a maximum downward shift of 5 meV, far below the observed maximum shift of 18 meV.

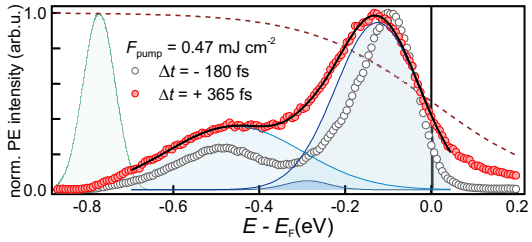

FIG. 2. Normalized EDCs at Γ before $\Delta t = 0$ fs (empty grey) and at $\Delta t = 365$ fs after (solid red) photoexcitation with 0.47 mJ/cm^2 at 110 K. The exemplary fit curve (black line) is composed of three Gaussian peaks (blue) multiplied by a Fermi-Dirac occupation distribution (red dashed), and convolved with a Gaussian accounting for the energy resolution (green).

The transient population of the VBs has been estimated from the area under the corresponding peak at each pump-probe delay. It should be noted that the electric field of the intense pump pulses might affect the spectral shape probed by ARPES. However, such effects occur only during the pump pulse duration [2] and could solely have an impact on our results at time delays ± 50 fs.

The band gap of TNS is approximately 0.3 eV [3]. In Ref. [4], this corresponds to the isobestic point in the optical data. From our ARPES data at equilibrium (without pump photons) and at 110 K, we find that the upper VB lies at $E - E_F$ = -0.11 eV, which is smaller than half the band gap value. This suggests a slight p-doping of our sample.

This assertion about the p-doping of our sample is further supported by a Hall resistivity measurement performed on another sample from the same growth batch (see Fig. 3), which confirms that the Hall resistivity is hole-like (positive) on the whole temperature range displayed here.

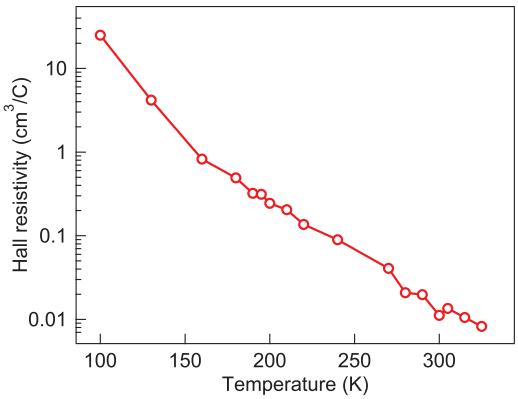

FIG. 3. Hall resistivity of our TNS samples.

Theoretical modeling

We investigate the nonthermal state of the EI by considering a one-dimensional two-band system of spin-less fermions (spin-degrees of freedom are not included) with direct band gap, $H = H_0 + H_{\rm int}$, where the noninteracting part is

$$H_0 = \sum_{k,\alpha} (\epsilon_{k,\alpha} + \eta_\alpha) c^\dagger_{k,\alpha} c_{k,\alpha},$$

with the band dispersion $\epsilon_{k,1(2)} = -(+)2t_0 \cos(k)$. The $c_{k,\alpha}$ denote the annihilation operators for an electron with momentum k in orbital $\alpha = 1, 2$. The bare band splittings $\eta_{1,2}$ are chosen such that band 1(2) is totally occupied (unoccupied). The hopping parameter t_0 is chosen such that the ground state dispersion in the unordered state matches the experimental one. For the interaction we consider a local density-density CIA of the form

$$H_{\rm int} = \frac{1}{2} \sum_i U n_{i,1} n_{i,2}.$$

We determined the interaction U by the comparison of calculated and equilibrium ARPES spectra in the ordered and unordered state. Explicitly, for the ground state calculations, we used $t_0 = 0.26$ eV, $U/t_0 = 3.0$ and the relative bare band splitting $(\eta_2 - \eta_1)/t_0 = 2.1$.

The excitonic instability arises because of the attractive CIA between the electrons in the upper band and the holes in the lower band, leading to a condensation of the excitons which are formed across the direct band gap. The order parameter of the condensate is

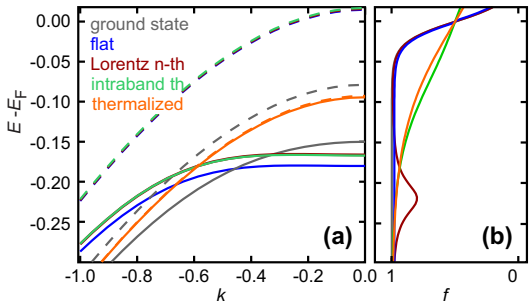

FIG. 4. (a) Comparison of the ground state dispersion relation to the ones obtained from different nonthermal distribution functions, namely in blue a constant population of holes (electrons), in dark red a dip (hump) in the Fermi-Dirac distribution function below (above) $E_{\rm F}$, respectively, in green the corresponding *intra*band thermalized distribution at elevated temperatures. The negative energy parts of the corresponding distribution functions are presented in panel (b).

$\rho_{12} = \langle c^\dagger_{k,1} c_{k,2}\rangle \neq 0$. In order to solve the problem we employ standard Hartree-Fock calculations based on the mean-field decoupling of the interaction term. The experimentally observed abrupt band gap narrowing is modeled by a reduction of the bare band splitting $\eta_2 - \eta_1$ between the VB and CB. The effect of the nonthermal distribution on the band gap size Δ is determined from the self-consistent Hartree-Fock calculation. In order to show that the conclusions do not depend on the particular choice of the distribution function, we compared several parametrizations of the nonthermal distribution function, see Fig. 4(b): (i) additional constant population of holes (electrons), (ii) Lorentzian peak (dip) in the Fermi-Dirac distribution function below (above) $E_{\rm F}$, namely $f_{\rm nth}(\epsilon, A, \overline{E}) = f_{\rm FD}(\epsilon, 0) + A\gamma^2/((\epsilon - \overline{E})^2 + \gamma^2)$, where $f_{\rm FD}(\epsilon, \mu)$ is the Fermi-Dirac distribution, A is the amplitude, γ the width and $\overline{E}$ the center position of the Lorentzian peak (dip), (iii) intraband thermalized distributions at elevated temperatures.

As shown in Fig. 4(a), for all these nonthermal distributions with the same excitation density n_{ex} the band gap at Γ is enhanced except for the *fully* thermalized one (solid orange in Fig. 4(e)). This means that photoexcitation of an EI can result in a transient enhancement of the order parameter, if thermalization is sufficiently delayed by, for instance, the presence of the band gap, consistently with the experimental observations at later time delay.

The theory that we present does not aim at realistically reproducing the experimental setup, including the photoexcitation and all possible relaxation processes. We rely on the separation of the time scales for the relaxation, and assume that the intraband electron-electron scattering leads to a fast relaxation and thermalization within each band, while the thermalization between the bands is mediated by electron-phonon interactions whose characteristic time is much longer. This leads to a nonthermal distribution function which exists in a relatively long time-window. The mean-field analysis is well suited to describe the state of the system, i.e., its band structure and order parameter, in the presence of such a nonthermal electron distribution. In order to simulate the relaxation and thermalization and therefore predict the precise time-dependent form of the nonthermal distribution function, however, one needs to include processes like electron-electron and electron-phonon scattering in the real-time description, which can be obtained by more advanced descriptions beyond mean-field, such as GW or DMFT. In these approaches, however, the timescales that one can reach are limited by the large cost in memory and computer time. Therefore, there is a need to develop new techniques to describe the long time behavior that includes the relaxation and thermalization dynamics, which is a challenging problem for future theoretical studies.

* monney@physik.uzh.ch

[1] The separate shifts of B and C exhibit the same qualitative behavior (not shown).
[2] F. Mahmood, C.-K. Chan, Z. Alpichshev, D. Gardner, Y. Lee, P. Lee, and N. Gedik, Nature Phys. **12**, 306 (2016).
[3] Y. Okamura, Private communication (2014).
[4] Y. Lu, H. Kono, T. Larkin, A. Rost, T. Takayama, A. Boris, B. Keimer, and H. Takagi, Nature Commun. **8**, 14408 (2017).